PHYSICAL REVIEW B

CONDENSED MATTER

THIRD SERIES, VOLUME 43, NUMBER 13 PART A 1 MAY 1991

Nucleation kinetic studies of a europium-doped aluminosilicate glass: Low-frequency inelastic scattering and fluorescence line narrowing

J. A. Capobianco and P. P. Proulx
Department of Chemistry and Biochemistry, Concordia University, 1455 de Maisonneuve Boulevard West, Montréal, Québec, Canada H3G 1M8

B. Andrianasolo and B. Champagnon
Physico-Chimie des Materiaux Luminescents, Université de Lyon I, 69622 Villeurbanne, France
(Received 26 November 1990)

An investigation of low-frequency inelastic scattering and fluorescence line narrowing has revealed the role of Eu^{3+} in the nucleation process. Analysis of the results has shown that the Eu^{3+} accelerates nucleation; however, it is not incorporated into the microcrystalline phase. Polarization studies have shown that the nucleating agents Eu^{3+} and Cr^{3+} modify the size of the microcrystallites and the symmetry of the vibrational eigenmodes. The results show that the vibrational eigenmodes for the Cr^{3+}-doped glass are mainly breathing modes, whereas for the Eu^{3+}-doped and undoped glass they are spheroidal and/or torsional modes.

I. INTRODUCTION

In recent years, transparent glass ceramics have received considerable attention because of the interest in their potential in application in laser technology. In general, glass ceramics are defined as multiphase materials produced by the controlled crystallization of certain glass compositions. The unique property of transparent glass ceramics is that they contain crystals embedded in the amorphous phase (glass) whose size is such that Rayleigh scattering is negligible. Transparent glass ceramics are typically made from their precursor glasses by adding a nucleating agent and by following a suitable heat treatment. However, the relationship between the increase in the nucleation rate and the amorphous phase separation as a consequence of adding a nucleating agent is a complex and little understood process.[1] We will define a nucleating agent as any element which modifies during the nucleation process either the kinetics or the size of the particles.

Previous work[2] has suggested that the addition of Cr_2O_3 (nucleating agent) to an aluminosilicate glass (containing TiO_2, ZrO_2, and P_2O_5—all considered to be nucleating agents) modified the nucleation process. It was observed that the Cr^{3+} ions favor the formation of microcrystallites within the glassy matrix. This observation in itself is not unexpected; however, the presence of Cr^{3+} exclusively in the glass phase and not in the microcrystallites themselves is quite unusual. Furthermore, heat treatment of the chromium-doped and the undoped aluminosilicate glass produced, respectively a transparent and opaque glass ceramic.

Undoubtedly, a better understanding of the nucleation process and the role of the nucleating agents will be instrumental in the development of transparent glass ceramics for optical applications. In this paper we will report on the influence of Eu^{3+} on the nucleation process, using evidence from fluorescence-line-narrowing experiments (FLN) and low-frequency inelastic scattering (LOFIS). Fluoresence-line-narrowed spectra allow us to distinguish between Eu^{3+} in the glass and crystalline phase, whereas LOFIS enables us to obtain the frequency of the eigenmodes and the size of the microcrystallites.

II. THEORY: LOW-FREQUENCY INELASTIC SCATTERING

Low-frequency inelastic scattering is an excellent technique to study short- and long-range order in amorphous materials. Because of the short correlation length, a breakdown of the selection rules occurs[3] and the low-frequency spectrum of amorphous materials is dominated by the so-called "boson peak." Duval *et al.*[4] have shown that, in addition to the boson peak, Stokes and anti-Stokes bands appear very close to the Rayleigh line. These bands are related to the frequency of the eigenmodes of the microcrystallites in the glass matrix. In

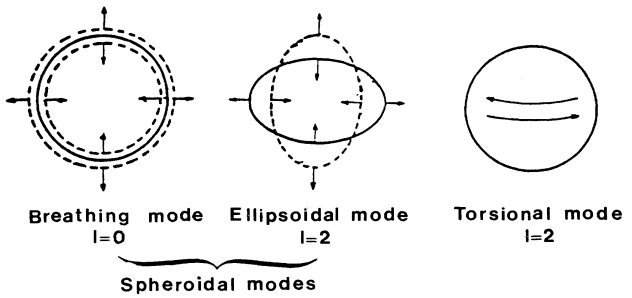

FIG. 1. Vibrational modes of a spherical particle.

what follows we will give an account of some theoretical aspects of LOFIS that are pertinent to this paper.

The movement of an elastic isotropic body is given by the Helmholtz equation

$$\rho\partial_t^2\mathbf{D}=(\lambda+\mu)\nabla(\nabla\mathbf{D})+\mu\nabla^2\mathbf{D} , \quad (1)$$

where $\mathbf{D}$ is the displacement vector, ρ is the density, and λ and μ are the Lamé coefficients. The solution of Eq. (1) gives a set of equations characteristics of a vibrating sphere,[5] for which two types of modes are distinguished: spheroidal and torsional. The spheroidal models are characterized by an angular momentum $l=0$ or 2, which correspond, respectively, to the breathing and ellipsoidal modes (Fig. 1). These modes are Raman active. The torsional Raman-active modes are characterized by an angular momentum $l=2$.

The vibrational energies of the torsional and ellipsoidal modes for a spherical body are given by

$$\omega_2^t=\omega_2^s=Sv_t/2ac , \quad (2)$$

where ω_2^t and ω_2^s are the torsional and ellipsoidal energies, respectively, v_t is the transversal sound velocity, S is a shape factor equal to 0.80 and 0.84, respectively for the torsional and ellipsoidal modes in the case where $v_l/v_t=\sqrt{3}$, c is the velocity of light in vacuum, and $2a$ is the diameter of the particle. The torsional and ellipsoidal modes correspond to vibrations which depolarized the incident light.

The equation for the vibrational energies of the breathing modes may be written as

$$\omega_0^s=Sv_1/2ac , \quad (3)$$

where S (defined previously) is equal to 0.82 and v_1 is the longitudinal sound velocity. In the samples studied the longitudinal and transversal sound velocities are 6490 and 3790 $\mathrm{m\,s^{-1}}$, respectively. Therefore, the energies of the vibrational modes calculated from Eq. (3) appear at a different energy from those calculated with use of Eq. (2). The breathing modes behave differently than the torsional or ellipsoidal modes with respect to polarization. For example, if the electric field of the polarized excitation light is in the direction of the observation, the spheroidal breathing will not give rise to inelastic scattering.

III. EXPERIMENT

The aluminosilicate glass (base glass) ($Li_2O\cdot Al_2O_3$-SiO_2-P_2O_5-ZrO_2-TiO_2) was prepared by Schott Glass, Mainz, Germany. This glass is the precursor for the glass-ceramic Zerodur (Schott).[6] The base glass was doped with 0.39 wt % Eu_2O_3 or 0.1 wt % Cr_2O_3. Four pieces of the base glass were treated for 10 h at 720 °C, 23 h at 720° C, 13 h at 800 °C and 48 h at 750 °C.

A 6-W Spectra Physics 2020 argon-ion laser provided the 514.5-nm excitation (400 mW) for the low-frequency inelastic-scattering experiments. The spectra were recorded with use of a Jobin-Yvon U1000 double-monochromator using a maximum slit of 100 μm. Light scattered at $\pi/2$ from the incident beam was monitored with an Hamamatsu GaAs photomultipler operating in the photon-counting mode.

In order to distinguish between the breathing and the torsional or ellipsoidal modes, two polarizations of the incident light were considered. The excitation wave vector is usually in the x direction with two possible orientations of the electric field, horizontal or vertical. The scattered light was observed in the y direction. The efficiency of the gratings in the y direction is 80% for vertical polarization and 40% for the horizontal polarization for the 514.5-nm excitation line.

A Spectra Physics 375 dye laser operating with Rhodamine-6G (10^{-3} mol/dm^3 in ethylene glycol) pumped by a Coherent Inc. CR-18 argon-ion laser was used for excitation of the FLN spectra. The laser has a typical linewidth of 2-$\mathrm{cm^{-1}}$ full width at half maximum (FWHM) over the tuning range 575–581 nm used in this work. The spectra were recorded with a Jarrel-Ash 1-m Czerny-Turner double monochromator using a maximum slit of 150 μm. The fluorescence signal was monitored with an RCA-C31034-02 photomultiplier in the photon-counting mode and recorded under computer control using a Stanford SR 465 software data-acquisition and-analysis system. The data were acquired at liquid-nitrogen temperature (77 K) using a continuous flow cryostat built at Concordia University.

IV. RESULTS AND DISCUSSION

A. Low-frequency inelastic scattering

The LOFIS spectra in the region below 180 $\mathrm{cm^{-1}}$ for the samples studied are shown in Figs. 2 and 3. Characteristic of the spectra are the boson peaks (above 60 $\mathrm{cm^{-1}}$) and the low-frequency peaks (indicated by arrows). The nature and origin of this spectral characteristic of amorphous material has received considerable attention.[7,8] Recently, Duval *et al.*[9] have interpreted the boson peak as reflecting the maximum of the effective density of states, $g(\omega)$. Based on this interpretation, a shift in the position (lower frequency) indicates an increase in the size of the "blobs" which make up the glass. These "blobs" may be considered as groups which make up the glass.

A comparison between the spectra (Figs. 2 and 3) of the samples heat treated for 10 and 23 h show that those heated for 23 h have (i) a more prominent boson peak and

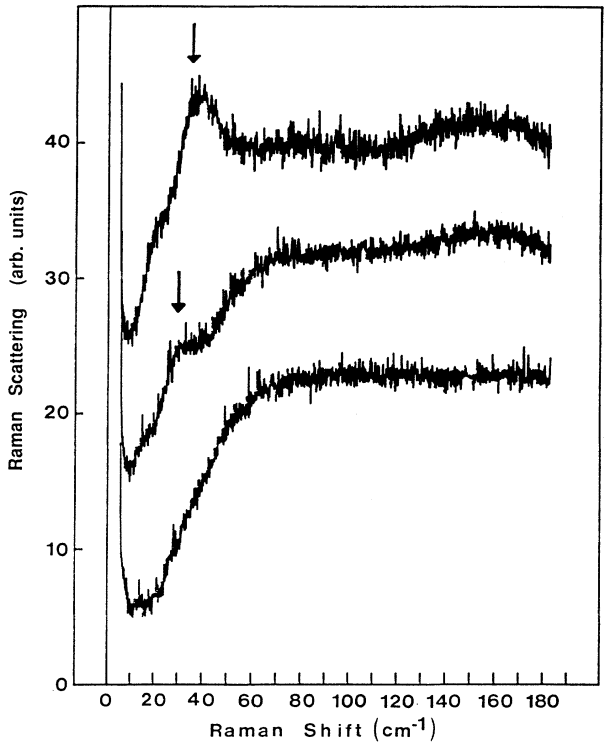

FIG. 2. Low-frequency inelastic-scattering spectra of Cr^{3+}-doped (top), Eu^{3+}-doped (middle), and undoped (bottom) aluminosilicate glass. Samples heat treated for 10 h at 720 °C.

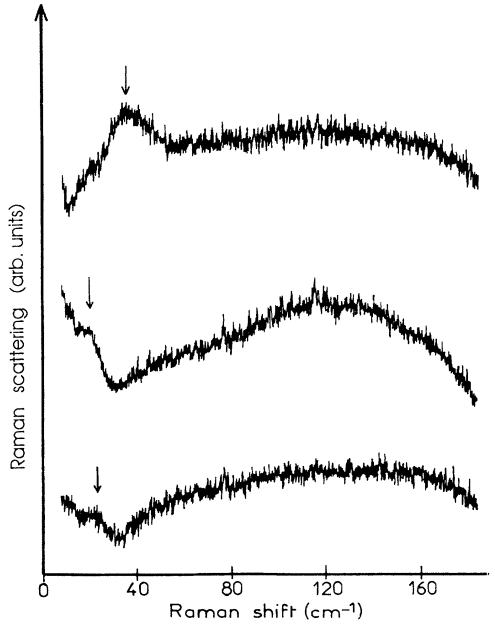

FIG. 3. Low-frequency inelastic-scattering spectra of Cr^{3+}-doped (top), Eu^{3+}-doped (middle), and undoped (bottom) aluminosilicate glass. Samples heat treated for 23 h at 720 °C.

TABLE I. Peak position (cm^{-1}) and diameter (nm) of crystallites in the chromium- and europium-doped samples.

Sample		$P1$ (cm^{-1})	$P2$ (cm^{-1})	$2a$ (nm)
Chromium doped	10 h, 720 °C	20	38	4.9
	23 h, 720 °C	20	36	5
Europium doped	10 h, 720 °C	15	34	6
	23 h, 720 °C	10	19	9.7

(ii) its position is shifted. These observations lead us to conclude that either the blobs have decreased in size, or phase separation occurred during the heat treatments.

Another characteristic of the spectra (Figs. 2 and 3) is the low-frequency peak (<40 cm^{-1}). Heat treatment of the samples leads to the formation of microcrystallites. From the position of the peaks (Table I) we can calculate the diameter of the crystallites, using Eqs. (2) and (3). The results are shown in Table I and are summarized as follows.

(i) All samples (doped or undoped) show two low-frequency peaks.

(ii) The Eu^{3+}-doped sample (heat treated for 10 h) contains microcrystallites which have a larger diameter than the Cr^{3+}-doped samples.

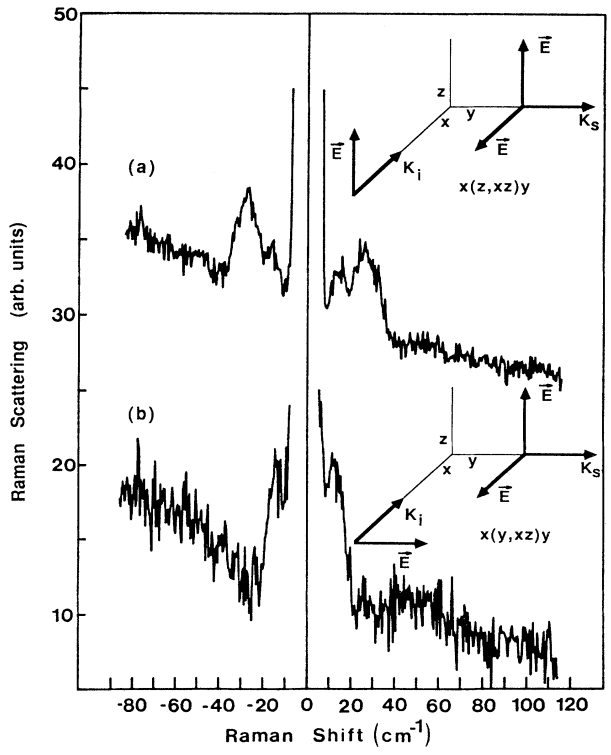

FIG. 4. Stokes and anti-Stokes low-frequency inelastic-scattering bands of Eu^{3+}-doped aluminosilicate glass obtained with (a) vertical polarization and (b) horizontal polarization. Sample heat treated for 48 h at 750 °C.

(iii) The diameter of the microcrystallites for the Cr^{3+}-doped sample heat treated for 23 h remain approximately the same as those found in the sample heat treated for 10 h. However, the microcrystallites in the Eu^{3+}-doped samples continue to grow as a function of time.

Seeking a suitable explanation for the fact that two low-frequency peaks are observed, we considered two possibilities: (i) The peaks correspond to two size distributions of the microcrystallites, or (ii) they correspond to different eigenmodes of a single size distribution.

We mentioned in the theoretical section that the spheroidal breathing modes and the torsional and ellipsoidal modes behave differently with respect to polarization. Therefore, we examined the effect of polarization on the two peaks. Figure 4 shows the Stokes and anti-Stokes bands when the electric field of the incident light is either vertical [Fig. 4(a)] or horizontal [Fig. 4(b)]. We observe that, with a vertical polarization, two peaks with maxima at 25 and 14 cm^{-1} from the Rayleigh line were found and that the peak at 25 cm^{-1} was more intense. However, with a horizontal polarization only one peak with a maximum at 14 cm^{-1} was found. It is clear (see Sec. II) that the peak at 25 cm^{-1} [Fig. 4(a)] can be assigned to the spheroidal breathing modes and that, at 14 cm^{-1} [Fig. 4(b)], it can be assigned to the torsional or ellipsoidal modes. The diameter of the microcrystallites (in both polarization) was calculated to be 3.5 nm. This leads us to conclude that the two peaks correspond to a single size distribution of microcrystallites with eigenmodes of different symmetry.

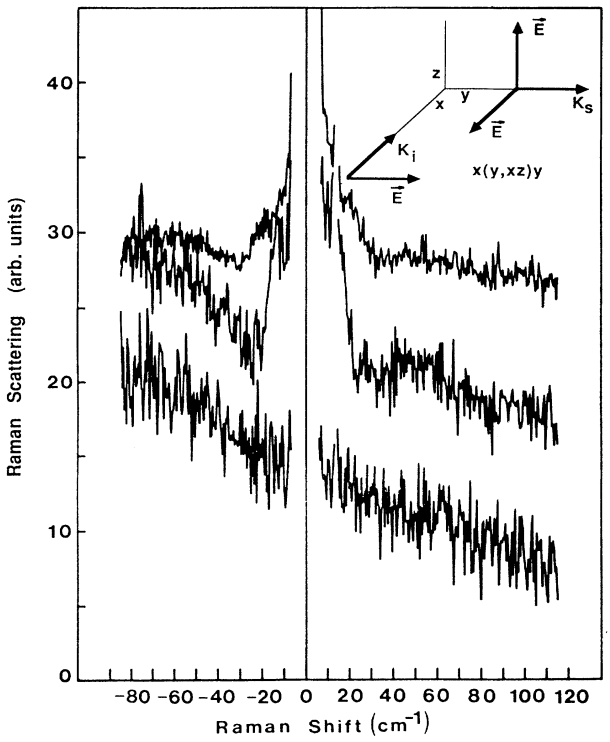

FIG. 5. Stokes and anti-Stokes low-frequency inelastic-scattering bands of undoped (top), Eu^{3+}-doped (middle), and Cr^{3+}-doped (bottom) aluminosilicate glass, obtained with horizontal polarization. Samples heat treated for 48 h at 750 °C.

Undoubtedly, another interesting and important fact to consider is whether the microcrystallites grown in the chromium-doped or undoped glass behave the same as those grown in the europium-doped glass with respect to polarization. Figure 5 shows LOFIS spectra of the undoped, chromium-doped and europium-doped samples obtained with the electric field in the y direction (horizontal polarization). The salient and most striking result is that the spectrum for the chromium-doped sample heat treated for 48 h at 750 °C does not show a low-frequency peak. The absence of this peak indicates that the introduction of a dopant ion in the glass not only modifies the size of the microcrystallites (as shown previously), but also the symmetry of the vibrational eigenmodes. We conclude that the vibrational eigenmodes for the chromium-doped glass are mainly breathing-modes, whereas, for the europium-doped and undoped glass, they are spheroidal and/or torsional modes.

B. Fluorescence line narrowing

In previous papers,[10–12] we showed that fluorescence-line-narrowing techniques can provide a powerful tool to study the local environment around the fluorescent ion (Eu^{3+}), phase separation, and crystallization behavior in glass or glass ceramics. We applied this technique to the Eu^{3+}-doped sample to determine whether europium partitions into the glass and/or crystalline phase and its role in the nucleation process.

The line-narrowed emission spectra of the untreated and heat-treated glass, excited at various wavelengths

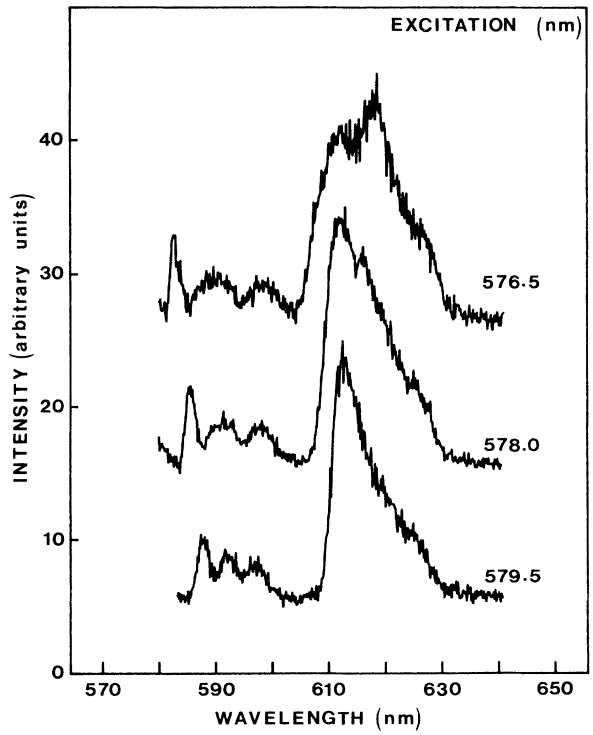

FIG. 6. Emission spectra of Eu^{3+} in aluminosilicate glass at 77 K using different excitation wavelengths.

within the $^5D_0 \rightarrow {}^7F_0$ emission bands, are shown in Fig. 6. The emission bands of the spectra obtained are characteristic of those produced by glasses,[10–11,13–15] indicating that the Eu^{3+} ion is in the glassy phase. If this were not the case, we would expect the spectra to show both inhomogeneously broadened glasslike and sharp crystallike Eu^{3+} fluorescence as observed for europium-containing phosphotungstate[16] and sodium calcium aluminum titatium silicate glass ceramics.[11]

This result is not unreasonable if we consider that the emission spectra of Nd^{3+} in a lithium aluminosilicate glass ceramic[17] has been reported to be similar to that of silicate glass, indicating that the rare-earth ion was in the glassy phase. This is very reasonable because the crystalline phase of a lithium aluminosilicate glass ceramic does not have an appropriate site for incorporating the trivalent rare earth.[18–20] In the aluminosilicate glass ceramic studied, the crystalline phase has been shown to be $ZrTiO_4$,[21] which does not have an appropriate site for the Eu^{3+} ion.

V. CONCLUSIONS

The present work has clarified the role which europium plays in the nucleation process of an aluminosilicate glass. We have shown that europium accelerates the nucleation process, and that it does not limit the size of the microcrystallites. We have demonstrated, using polarization studies, that the Raman-active vibrational modes of the microcrystallites are (i) spheroidal breathing and torsional and/or ellipsoidal modes if Eu^{3+} is present, and (ii) mainly breathing modes if Cr^{3+} is present. Fluorescence-line-narrowing results showed that, although Eu^{3+} induces nucleation, it is, however, not incorporated into the microcrystallites. We postulate that Eu^{3+} plays a role at the interface between the microcrystallites and the amorphous phase. The fact that neither Eu^{3+} or Cr^{3+} enters the microcrystalline phase confirms the importance of amorphous phase separation in the nucleation process.

ACKNOWLEDGMENTS

The authors gratefully acknowledge the Natural Sciences and Engineering Research Council of Canada, the Faculty of Arts and Science of Concordia University and the Centre National de la Recherche Scientifique of France for financial support. We also acknowledge the Government of France and Provincial Government Québec for their financial support. We thank E. Rodek, of Schott Glass, Mainz, Germany, who kindly provided us with the samples; and E. Duval, for very useful discussions.

[1]P. J. James, in *Glass and Glass-Ceramics,* edited by M. H. Lewis (Chapman and Hall, London, 1989), Chap. 3.
[2]B. Andrianasolo, B. Champagnon, and C. Esnouf, J. Non-Cryst. Solids **126**, 103 (1990).
[3]R. Shuker and R. W. Gammon, Phys. Rev. Lett. **25**, 222 (1970).
[4]E. Duval, A. Boukenter, and B. Champagnon, Phys. Rev. Lett. **56**, 2052 (1986).
[5]B. Andrianasolo, Ph.D. thesis, Université de Lyon I, 1990.
[6]V. Maier and G. Muller, J. Amer. Ceram. Soc. **70**, C176 (1987).
[7]B. Champagnon, B. Andrianasolo, A. Boukenter, E. Duval, and J. L. Rousset, Mater. Sci. Monogr. **60**, 342 (1989).
[8]B. Andriansolo, B. Champagnon, E. Duval, and C. Esnouf, in *Basic Features of the Glassy State,* edited by J. Colmenero and A. Alegria (World-Scientific, Singapore, 1990).
[9]E. Duval, A. Boukenter and A. Chibat, J. Phys. Condens. Matter **2**, 10227 (1990).
[10]J. A. Capobianco, P. P. Proulx, and N. Raspa, Chem. Phys. Lett. **160**, 591 (1989).
[11]J. A. Capobianco, T. F. Belliveau, G. Lord, D. J. Simkin, J. Tait, and P. J. Hayward, Phys. Rev. B **34**, 4204 (1986).
[12]J. A. Capobianco, P. P. Proulx, M. Bettinelli, and F. Negrisolo, Phys. Rev. B **42**, 5936 (1990).
[13]C. Brecher and L. A. Riseberg, Phys. Rev. B **13**, 81 (1976).
[14]C. Brecher, L. A. Riseberg, and M. J. Weber, Phys. Rev. B **18**, 5799 (1978).
[15]J. Hegarty, W. M. Yen, M. J. Weber, and D. H. Blackburn, J. Lumin. **18/19**, 657 (1979).
[16]H. Mack, G. Boulon, and R. Reisfeld, J. Lumin. **24/25**, 111 (1981).
[17]G. Muller and N. Neuroth, J. Appl. Phys. **44**, 2315 (1972).
[18]C. F. Ropp and J. Chrysochoos, J. Mater. Sci. **7**, 1090 (1972).
[19]C. F. Ropp and J. Chrysochoos, J. Phys. Chem. **77**, 1016 (1973).
[20]M. J. Weber (unpublished).
[21]A. Ramos and M. Gandais, J. Non-Cryst. Solids **100**, 471 (1990).